relevant to the problem of dioxygen reduction is the absence of $\mu$-oxo formation. Evaluation of $((TTOP)Fe)_2$ as a useful electrocatalyst is in progress.

**Acknowledgment.** We are grateful to Arden Boersma and Gregory Godziela for repetition of electrochemical measurements and synthetic procedures. Preliminary high-field NMR measurements were made at the Colorado State University Regional NMR Center, funded by National Science Foundation Grant No. CHE 78-18581. The Bruker WM-360 NMR spectrometer at the University of Iowa was purchased in part by NSF Grant No. CHE 82-01836. Support from the National Science Foundation, Grants CHE 79-10305 and CHE 82-09308 (H.M.G.), and the National Institutes of Health, Grants GM-28831 (H.M.G.) and HL-15627 (W.R.S.), is gratefully acknowledged.

**Registry No.** $((TTOP)Fe)_2$, 88200-64-0; $((TTOP)Fe)_2 \cdot 2C_7H_8$, 88200-65-1; (TTOHP)FeCl, 88200-66-2; (TPP)FeOPh, 76282-28-5.

**Supplementary Material Available:** Anisotropic temperature factors (Table IV), fixed hydrogen atom positions and isotropic temperature factors (Table V), and a listing of observed and calculated structure factor amplitudes (×10) (18 pages). Ordering information is given on any current masthead page.

Contribution from the Department of Chemistry, University of Iowa, Iowa City, Iowa 52242

# Carbon-13 and Deuterium NMR Spectroscopy of High-Spin Manganese(III) Porphyrin Halide and Pyridine Complexes

HAROLD M. GOFF* and ANDREW P. HANSEN

*Received September 8, 1982*

Carbon-13 NMR spectroscopic measurements have been performed for high-spin manganese(III) porphyrins to evaluate effects of axial ligand binding and to correlate isotropic shift patterns with d-orbital occupation. A qualitative description of unpaired spin delocalization mechanisms is offered. No particular ordering of resonances is apparent for $F^-$, $Cl^-$, and $I^-$ adducts, but absolute shift values for the $F^-$ complex are larger and approach those for the stronger field 4-methylpyridine ligand. Resonances for $\alpha$-pyrrole carbon atoms are downfield and cover a range from 383 to 492 ppm. Corresponding $\beta$-pyrrole carbon signals are upfield in the region from −72 to −166 ppm. The meso carbon signal exhibits a small upfield shift, which increases in magnitude with 4-methylpyridine displacement of the halide ligand. Previously elucidated carbon-13 shift correlations are consistent with predominant unpaired $\pi$-spin density at $\beta$-pyrrole and meso carbon sites of manganese(III) porphyrins. Negative $\pi$-spin density at the meso carbon atom is to be contrasted with earlier Hückel calculations that predict large positive spin density at this position. Deuterium NMR spectroscopy revealed large downfield shifts for $\alpha$- and $\beta$-deuterium atoms of coordinated pyridine-$d_5$. Corresponding carbon-13 signals are also far downfield. These observations are readily explained by transmission of $\sigma$-spin density from the singly occupied $d_{z^2}$ orbital to the axial pyridine ligand.

## Introduction

Nuclear magnetic resonance spectroscopy of paramagnetic complexes potentially can yield information about magnetic anisotropy, d-orbital occupation, unpaired spin delocalization mechanisms, and perturbations of electronic structure. Paramagnetic metalloporphyrins have been the subject of numerous proton NMR studies, and correlatons between shift patterns and d-orbital occupation are well-established.[1,2] Such results have important biological implications and applications. In physical–inorganic terms, metalloporphyrin complexes also provide a rigid, well-defined ligand system for developing a general understanding of carbon-13 paramagnetic shifts. The information content of carbon-13 spectra is especially great, but separation of the various shift contributions is correspondingly more difficult than is the case for proton spectra. The challenge to delineate carbon-13 shift mechanisms has inspired systematic examination of high-spin iron(III),[3-10] low-spin iron(III),[3,11-15] admixed-spin iron(III),[16] $\mu$-oxo dimeric iron(III),[3,4] high-spin iron(II),[17] and low-spin cobalt(II)[18] porphyrin complexes.

The work reported here focuses on using high-spin manganese(III) porphyrin complexes to test our expectations relating electronic structure with carbon-13 NMR shift patterns. Effects of changing the axial ligand are investigated. A qualitative description of unpaired spin delocalization mechanisms is offered on the basis of comparative carbon-13, proton, and deuterium NMR shift patterns. Results complement earlier proton NMR interpretations and theoretical calculations and at the empirical level could be used to distinguish the +3 oxidation state of manganese porphyrins.

## Experimental Section

Manganese(III) porphyrin complexes were prepared by the standard dimethylformamide reflux method.[19] A solution of the crude product in methylene chloride was shaken with 1 M aqueous sodium hydroxide, and the organic layer was subjected to column chromatographic purification on alumina. The resulting "hydroxo" manganese(III) porphyrin was converted to the halide complex by stirring a methylene chloride solution with the appropriate 1 M aqueous acid. Crystalline product was formed by addition of heptane to a concentrated methylene chloride solution of the manganese(III) porphyrin. Products were routinely vacuum-dried at 100 °C. Proton NMR spectra,[20,21] UV–vis spectra,[22] and thin-layer chromatography confirmed the identity and

(1) La Mar, G. N.; Walker, F. A. In "The Porphyrins"; Dolphin, D., Ed.; Academic Press: New York, 1979, Vol. IV, pp 61-157.
(2) Goff, H. M. In "Iron Porphyrins—Part I"; Lever, A. B. P., Gray, H. B., Eds.; Addison-Wesley: Reading, MA, 1982; pp 237-281.
(3) Goff, H. M.; Morgan, L. O. *Bioinorg. Chem.* **1978**, *9*, 61.
(4) Goff, H. *Biochim. Biophys. Acta* **1978** *542*, 348.
(5) Mispelter, J.; Momenteau, M.; Lhoste, J.-M. *J. Chem. Soc., Chem. Commun.* **1979**, 808.
(6) Phillippi, M. A.; Goff, H. M. *J. Chem. Soc., Chem. Commun.* **1980**, 455.
(7) Mispelter, J.; Momenteau, M.; Lhoste, J.-M. *J. Chem. Soc., Dalton Trans.* **1981**, 1729.
(8) Phillippi, M. A.; Baenziger, N.; Goff, H. M. *Inorg. Chem.* **1981**, *20*, 3904.
(9) Behere, D. V.; Mitra, S. *Proc. Indian Acad. Sci. Sect. X* **1982**, *91X*, 145.
(10) Goff, H. M.; Shimomura, E. T.; Phillippi, M. A. *Inorg. Chem.* **1983**, *22*, 66.
(11) Wüthrich, K.; Baumann, R. *Helv. Chim. Acta* **1973**, *56*, 585.
(12) Wüthrich, K.; Baumann, R *Helv. Chim. Acta* **1974**, *57*, 336.
(13) Goff, H. *J. Chem. Soc., Chem. Commun.* **1978**, 777.
(14) La Mar, G. N.; Viscio, D. B.; Smith, K. M.; Caughey, W. S.; Smith, M. L. *J. Am. Chem. Soc.* **1978**, *100*, 8085.
(15) Goff, H. M. *J. Am. Chem. Soc.* **1981**, *103*, 3714.
(16) Boersma, A. D.; Goff, H. M. *Inorg. Chem.* **1982**, *21*, 581.
(17) Shirazi, A.; Leum, E.; Goff, H. M. *Inorg. Chem.* **1983**, *22*, 360.
(18) Shirazi, A.; Goff, H. M. *Inorg. Chem.* **1982**, *21*, 3420.
(19) Adler, A. D.; Longo, F. R.; Varadi, V. *Inorg. Synth.* **1976**, *16*, 213.
(20) La Mar, G. N.; Walker, F. A. *J. Am. Chem. Soc.* **1973**, *95*, 6950.
(21) La Mar, G. N.; Walker, F. A. *J. Am. Chem. Soc.* **1975**, *97*, 5103.

0020-1669/84/1323-0321$01.50/0 

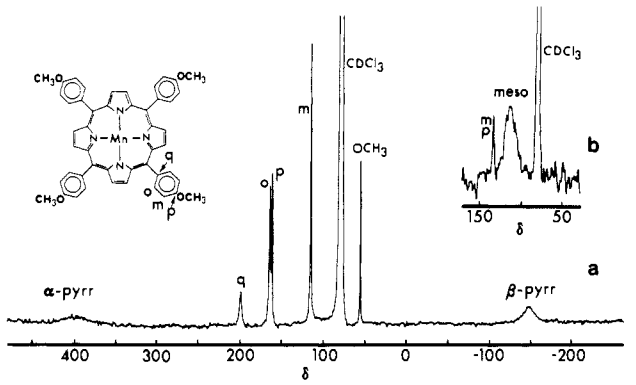


**Figure 1.** Proton-decoupled carbon-13 NMR spectra, $CDCl_3$ solvent, 34 °C, referenced to tetramethylsilane: (a) (TPP(*p*-$OCH_3$))MnCl, 0.05 M; (b) meso carbon-13-labeled (TPP)MnCl, 0.01 M.

**Table I.** Carbon-13 NMR Spectra of Chloromanganese(III) Porphyrin Species[a]

| | porphyrin derivative | | | | |
|---|---|---|---|---|---|
| carbon atom | TPP | TPP-(*m*-$CH_3$) | TPP-(*p*-$OCH_3$) | OEP | ETIO |
| quat phenyl | 203.2 | 203.3 | 201.0 | | |
| ortho phenyl | 165.9 | 166.0, 162.1 | 164.6 | | |
| meta phenyl | 130.4 | 140.0, 130.9 | 115.7 | | |
| para phenyl | 130.4 | 130.9 | 162.0 | | |
| phenyl methyl | | 23.0 | 56.3 | | |
| meso | 111[b] | *c* | *c* | *c* | *c* |
| α-pyrrole | 410 | 396 | 406 | 383 | 384 |
| β-pyrrole | −153 | −151 | −147 | −72 | −78, −97 |
| ring $CH_2$ | | | | −38.6 | −39.9 |
| ring $CH_3$ | | | | | −55.5 |
| ethyl $CH_3$ | | | | 166.9 | 166.8 |

[a] Manganese(III) porphyrin 0.02–0.05 M, $CDCl_3$ solvent, 34 °C, referenced to tetramethylsilane, in ppm. [b] For meso carbon-13-labeled TPP. [c] Signal not detected.

homogeneity of the products. The meso-carbon-13-labeled TPP[23] was prepared from 60 atom % benzaldehyde-α-$^{13}C$ (Merck).

A JEOL FX-90Q pulsed FT NMR instrument was used for proton (90 MHz), carbon-13 (22.5 MHz), and deuterium (13.7 MHz) measurements. For variable-temperature work carbon-13 spectra were recorded in the proton-coupled mode to avoid decoupler RF heating problems. Temperature calibration was performed by the Van Geet methanol thermometer method.[24] Carbon-13 spectral widths ranged from 20 to 40 kHz. Pulse repetition rates up to eight times per second permitted acquisition of adequate spectra in from 2 to 16 h (50 000 to 500 000 pulses). Solutions were generally saturated, and concentrations ranged from 0.02 to 0.05 M. The $CDCl_3$ solvent used for NMR studies was stirred with solid $K_2CO_3$, distilled, and stored over activated molecular sieves in the freezer.

## Results and Discussion

**Spectral Assignments.** A representative carbon-13 NMR spectrum of the (TPP(*p*-$OCH_3$))MnCl[23] species is presented in Figure 1. Carbon-13 spectral assignments for this and other complexes listed in Table I were made by a variety of methods. A signal at ~203 ppm was relatively invariant for three TPP phenyl-substituted species and was absent in the (OEP)MnCl[23] and (ETIO)MnCl[23] derivatives. The ~203 ppm signal was unsplit in proton-coupled spectra and in the spectrum of the meta phenyl-substituted compound. This information and the relative line width provide a reasonable assignment for this signal as the quaternary phenyl resonance. The signal near 165 ppm is that of a proton-bearing carbon atom, as was evident in a proton-coupled spectrum. This signal was split for the (TPP(*m*-$CH_3$))MnCl compound, indicating its assignment to the ortho phenyl carbon atom. Other phenyl carbon resonances are relatively sharp and approximate the values for known diamagnetic complexes. Assignment of both meta and para carbon resonances to the 130.9 ppm signal of (TPP)(*m*-$CH_3$))MnCl is further rationalized by resolution of two closely spaced signals at 50 °C.

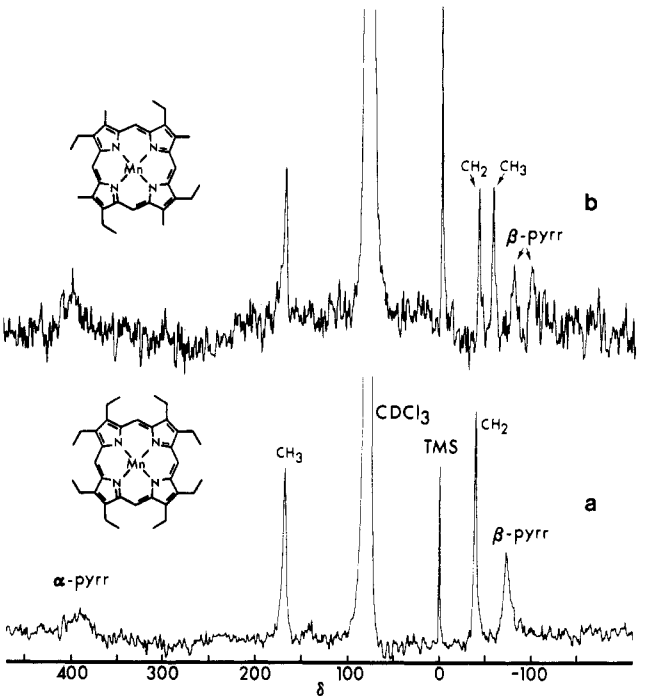


**Figure 2.** Proton-decoupled carbon-13 NMR spectra, $CDCl_3$ solvent, 34 °C, referenced to tetramethylsilane (TMS): (a) (OEP)MnCl, 0.03 M; (b) (ETIO)MnCl, 0.02 M.

Assignment of the meso carbon signal at 111 ppm was made unambiguously through incorporation of a carbon-13 label in (TPP)MnCl. A section of this spectrum is included in Figure 1b. Due to the large line width and overlap with the "wings" of strong solvent and phenyl signals, the meso carbon resonance was not reliably detected for natural isotopic abundance compounds.

The two remaining far upfield and far downfield signals must represent pyrrole carbon atoms. Aside from the expected order of line widths, the effect of pyrrole substituents can be used to assign the upfield signal to the β-pyrrole carbon atom. Thus, the downfield signal is found in a range of only 383–406 ppm as pyrrole substituents are changed from ethyl to hydrogen, whereas the upfield signal covers a range from −72 to −153 ppm. The β-pyrrole carbon resonance would be expected to be more sensitive to changes in pyrrole substituents. The extreme sensitivity is further indicated in Figure 2 where one β-pyrrole signal is observed at −72 ppm for (OEP)MnCl, whereas two signals at −78 and −97 ppm are seen in the (ETIO)MnCl spectrum. The two signals presumably correspond to β-pyrrole carbon atoms attached to ethyl and methyl groups, respectively.

Assignments of pyrrole substituents are readily made by examining spectra of both (OEP)MnCl and (ETIO)MnCl. Proton-coupled spectra reveal that signals at 167 and −39 ppm in Figure 2a represent proton-bearing carbon atoms, but large line widths preclude distinguishing triplet or quartet patterns. The spectrum for (ETIO)MnCl in Figure 2b exhibits two

(22) Boucher, L. J. *Coord. Chem. Rev.* **1972**, *7*, 289.
(23) Abbreviations: TPP, tetraphenylporphyrin; (TPP)MnCl, chloro(tetraphenylporphinato)manganese(III); (TPP(*p*-$OCH_3$))MnCl, chloro(tetrakis(*p*-methoxyphenyl)porphinato)manganese(III); (OEP)MnCl, chloro(octaethylporphinato)manganese(III); (ETIO)MnCl, chloro(etioporphinato I)manganese(III); 4-MePy, 4-methylpyridine.
(24) Van Geet, A. L. *Anal. Chem.* **1968**, *40*, 2227.

Table II. Axial Ligand Dependence of Carbon-13 Spectra for (TPP($p$-$OCH_3$))MnX[a]

| atom | axial ligand | | | |
|---|---|---|---|---|
| | $I^-$ | $Cl^-$ | $F^-$ | 4-MePy |
| quat phenyl C | 208.0 | 201.0 | 202.1 | 253.5 |
| ortho phenyl C | 161.7 | 164.6 | 159.6 | 94.0 |
| meta phenyl C | 116.2 | 115.7 | 116.3 | 111.8 |
| para phenyl C | 159.1 | 162.0 | 162.2 | 158.2 |
| phenyl $OCH_3$ C | 56.3 | 56.3 | 56.9 | 55.9 |
| meso C | b | b, 111[c] | b | b, 20[d] |
| $\alpha$-pyrrole C | 403 | 406 | 430 | 492 |
| $\beta$-pyrrole C | −144 | −147 | −155 | −166 |
| pyrrole H | −25.7 | −21.9 | −18.6 | −29.3 |

[a] Manganese(III) porphyrin 0.04–0.05 M, $CDCl_3$ solvent, 34 °C, referenced to tetramethylsilane, in ppm. [b] Signals not detected for natural abundance sample. [c] Value for meso carbon-13-labeled (TPP)MnCl, 0.01 M. [d] Value for meso carbon-13-labeled (TPP)MnCl in neat 4-methylpyridine.

signals in the same positions, along with an additional resonance at −55.5 ppm. This upfield signal must be that for the ring methyl carbon atom, and an expected common shift mechanism for the ring methylene group leads to assignment of the −39 ppm signal. The remaining 167 ppm signal is thus assigned to the methyl carbon atom of the ethyl group.

**Variable-Temperature Measurements.** Carbon-13 spectra for (TPP($p$-$OCH_3$))MnCl were recorded over the practical temperature range of the $CDCl_3$ solvent. Results are presented as Curie plots in Figure 3. Isotropic shifts were calculated using (TPP)$Co^{III}$ complexes[15] and the metal-free porphyrin as diamagnetic reference compounds. Meso carbon-13-enriched (TPP)MnCl was utilized to obtain the meso carbon values.

Significant deviations from curie law behavior are apparent in Figure 3 in the form of non-zero intercepts and nonlinearity for phenyl-carbon plots. Results for the $\beta$-pyrrole proton signal are also included, and the 15 ppm intercept for this signal is reasonably consistent with the previously reported value of 13 ppm.[21] The $\beta$-pyrrole carbon signal shows relatively small deviations from Curie law behavior in comparison with $\alpha$-pyrrole carbon and meso carbon resonances. Lack of Curie law correspondence is surprising in view of the rather ideal spin-only magnetic moments of 4.8–4.9 $\mu_B$ reported for various manganese(III) porphyrins.[22,25] Zero-field-splitting values are also very small and thus should not contribute measureable second-order temperature effects.[25,26] Dipolar shifts are too small for high-spin manganese(III) porphyrins[21] to directly account for nonlinearity due to possible aggregation at low temperatures. However, aggregation or solvation effects at low temperature could change substantially the axial ligand interaction. In this regard it should be noted (vide infra) that the nature of the axial ligand does indeed influence the NMR shift values. Variation of axial ligands is associated with significant chemical shift changes for meso, quaternary phenyl, ortho phenyl, and $\alpha$ carbon atoms. These resonances likewise exhibit the largest deviations from Curie law behavior (Figure 3). An aggregation mechanism appears less viable than other possibilities, as the meso carbon resonance exhibits the largest Curie law deviation, yet this signal was monitored for a solution 0.01 M in manganese(III) porphyrin. Other variable temperature spectra were recorded for a 0.05 M solution.

**Axial Ligand Dependence.** Effects of varying the axial ligand are demonstrated for (TPP($p$-$OCH_3$))MnX in Table II. Proton NMR spectra have previously been reported for the halide complexes and for a pyridine adduct.[21] Pyrrole

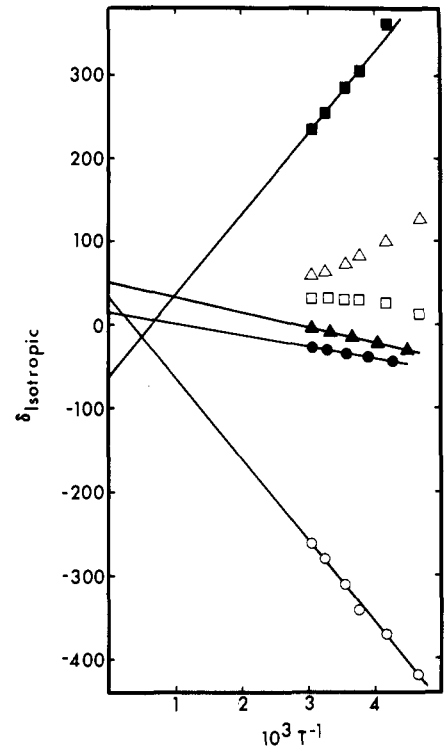


**Figure 3.** Curie law plot for (TPP($p$-$OCH_3$))MnCl, 0.05 M, $CDCl_3$ solvent: (○) $\beta$-pyrrole carbon; (●) $\beta$-pyrrole hydrogen; (□) ortho phenyl carbon; (△) quaternary phenyl carbon; (■) $\alpha$-pyrrole carbon; (▲) meso carbon of meso carbon-13-labeled (TPP)MnCl, 0.01 M.

proton resonance values (measured on samples used for carbon-13 NMR) listed in Table II are equivalent to those in the literature, thus confirming the integrity of the species examined here.

Correlations between carbon-13 shift values and zero-field splitting have been elucidated for high-spin iron(III) porphyrin complexes.[10] The ordering of selected chemical shift values also seemingly reflects the ligand-field strength of axial ligands. Among the halides the ordering of $D$ is $F^- < Cl^- < Br^- < I^-$ for iron complexes.[26,27] Zero-field splittings are smaller and negative for manganese(III) porphyrins,[25,26] and the limited magnetic measurements for $Br^-$ and $Cl^-$ complexes preclude extensive discussions about any relation to carbon-13 NMR shifts. It may be concluded from Table II that no consistent ordering of carbon-13 signals is apparent for $I^-$, $Cl^-$, and $F^-$ complexes. The spectrum of the fluoride complex is distinctive as compared with spectra of the other two halide derivatives. The largest differences are seen in pyrrole carbon shifts, which increase in absolute terms for the fluoride complex. These enhanced isotropic shifts are in the same direction as those for the even stronger field 4-methylpyridyl complex (Table II).

A recent electrochemical study has revealed coordination of manganese(III) porphyrins by a single nitrogenous base such as pyridine.[28] No evidence was found for bis ligation by a combination of pyridine and chloride ion in solution, although this is the situation in the solid state.[29] It was of interest to examine the carbon-13 NMR spectrum of a nitrogen-coordinated complex and 4-methylpyridine was chosen due to its relatively larger binding constant. Use of the iodide complex of (TPP($p$-$OCH_3$))$Mn^{III}$ further guaranteed 4-methylpyridine displacement of the weakly binding iodide ligand. Identical carbon-13 spectra at 4-methylpyridine concentrations

(25) Behere, D. V.; Mitra, S. *Inorg. Chem.* **1980**, *19*, 992.
(26) Brackett, G. C.; Richards, P. L.; Caughey, W. S. *J. Chem. Phys.* **1971**, *54*, 4383.
(27) Behere, D. V.; Birdy, R.; Mitra, S. *Inorg. Chem.* **1981**, *20*, 2786.
(28) Kadish, K. M.; Kelly, S. *Inorg. Chem.* **1979**, *18*, 2968.
(29) Kirner, J. F.; Scheidt, W. R. *Inorg. Chem.* **1975**, *14*, 2081.

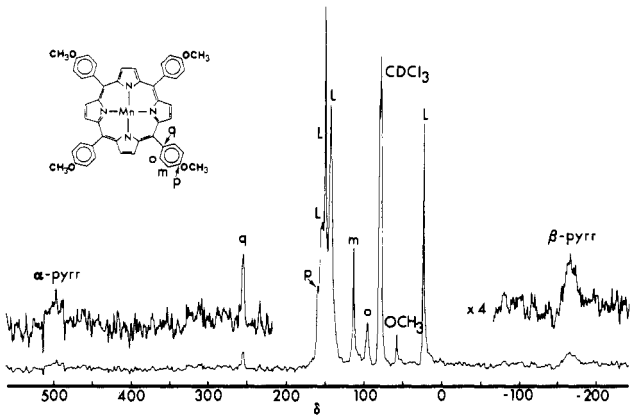


**Figure 4.** Proton-decoupled carbon-13 NMR spectrum of (TPP($p$-$OCH_3$))Mn(4-MePy)$^+$: manganese(III) porphyrin added as (TPP-($p$-$OCH_3$))MnI, 0.04 M; total 4-methylpyridine, 0.5 M; $CDCl_3$ solvent, 34 °C, referenced to tetramethylsilane.

of 0.5 and 3.0 M demonstrated that coordination was indeed complete at the lower concentration. A representative spectrum is shown in Figure 4. As noted previously, the pyrrole-carbon shifts for the nitrogen-coordinated complex are appreciably greater than for simple anionic complexes. The meso carbon resonance also exhibits a significant upfield shift to 20 ppm (for meso-labeled (TPP)MnCl in neat 4-methylpyridine), and as a consequence the attached quaternary-phenyl signal is shifted some 50 ppm further downfield than is the case for halide derivatives.

**NMR Spectroscopy of Coordinated Pyridine.** Rapid ligand exchange is apparent in the proton NMR spectra of manganese(III) porphyrin solutions containing excess pyridine or 4-methylpyridine. Aromatic proton signals for excess ligand are broadened and shifted downfield slightly, but large line widths and overlap with porphyrin phenyl signals preclude reliable calculation of coordinated chemical shift values. In addition, coordinated ligand signals were not detected by proton NMR spectroscopy for a $CDCl_3$ solution containing (TPP)MnCl and pyridine at −56 °C.

This problem was solved through use of deuterium NMR spectroscopy. Deuterium NMR has particular advantages in that the only signals observed are those from the deuterium-enriched molecule. Chemical shifts are expected to be the same as those for the proton, and furthermore in a paramagnetic environment deuterium signals may be up to 42 times sharper than proton signals.[30] (Poorer dispersion of deuterium signals means that the gain in resolution is only a factor of about six.[31,32]) Results for solutions containing (TPP)MnCl and varying concentrations of pyridine-$d_5$ are shown in Figure 5. Movement of pyridine signals toward the free-ligand position with increasing pyridine concentration is indicative of exchange in the fast limit. At −56 °C these signals had broadened significantly and shifted further downfield, but individual coordinated signals were not observed. At −85 °C the spectral result shown in Figure 6 was obtained. On the basis of shift directions noted in Figure 5, the far downfield signals at 180 and 109 ppm are assigned to the $\alpha$- and $\beta$-deuterium atoms of coordinated pyridine-$d_5$. These signals have respective line widths of ~1000 and 200 Hz. The $\gamma$-pyridine signal is shifted only very slightly (1–2 ppm) upfield and is not resolved from the broad free-pyridine signals in Figure 6 (apparent overlap of free-pyridine signals is due to broadening at very low temperature—a 20-Hz exponential-

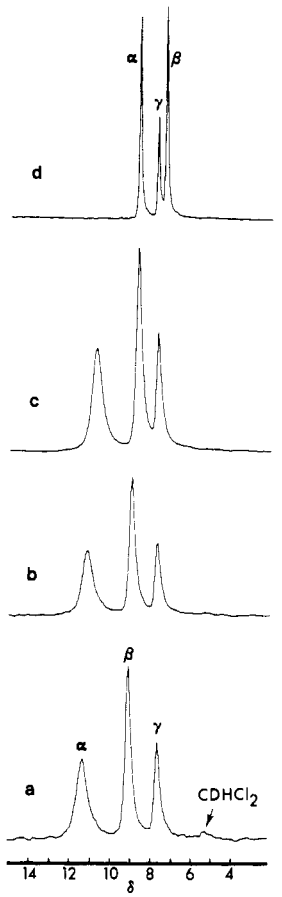


**Figure 5.** Deuterium NMR spectra of pyridine-$d_5$, $CH_2Cl_2$ solvent, 34 °C, referenced to tetramethylsilane ($CDHCl_2$ signal used as secondary reference): (a) pyridine-$d_5$ 0.05 M, (TPPMn)Cl, 0.03 M; (b) pyridine-$d_5$, 0.10 M, (TPP)MnCl, 0.03 M; (c) pyridine-$d_5$, 0.25 M, (TPP)MnCl, 0.03 M; (d) pyridine-$d_5$, 0.25 M.

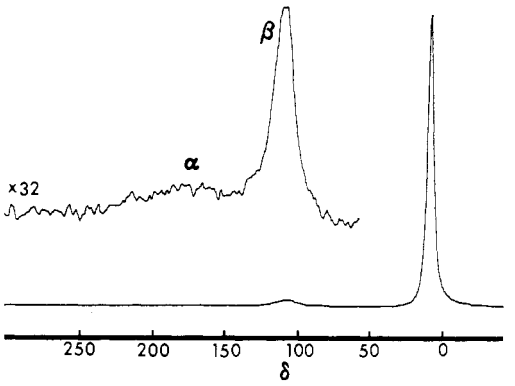


**Figure 6.** Deuterium NMR spectrum of pyridine-$d_5$ coordinated to TPPMn$^+$: $CH_2Cl_2$ solvent, −85 °C, manganese(III) porphyrin, 0.03 M, total pyridine-$d_5$ concentration, 0.25 M, referenced to tetramethylsilane.

multiplication broadening factor has been applied to this spectrum). If Curie law behavior is assumed, at 34 °C the coordinated pyridine $\alpha$- and $\beta$-deuterium resonances are expected at 114 and 70 ppm, respectively.

Relative concentrations of free and coordinated pyridine may be estimated from the spectra in Figure 5 using the coordinated resonance values, $\delta_c$, and the well-known mole-fraction-weighted relationship

$$\delta_{obsd}[Py]_T = \delta_f[Py] + \delta_c[(TPP)MnPy^+] \quad (1)$$

where $\delta_{obsd}$ is the observed resonance for a total pyridine concentration $[Py]_T$, $\delta_f$ is the resonance value for the free

(30) Swift, T. J. In "NMR of Paramagnetic Molecules"; La Mar, G. N., Horrocks, W. DeW., Holm, R. H., Eds.; Academic Press: New York, 1973; pp 53–83.
(31) Johnson, A.; Everett, G. W.; Jr. *J. Am. Chem. Soc.* **1972**, *94*, 1419.
(32) Wheeler, W. D.; Kaizaki, S.; Legg, J. I. *Inorg. Chem.* **1982**, *21*, 3248.

ligand, and [Py] and [(TPP)MnPy$^+$] reflect concentrations at equilibrium. Calculations reveal that only 4–17% of (TPP)Mn$^+$ is in the pyridine-ligated form for the conditions given in Figure 5. For the accepted equilibrium[28]

$$(TPP)MnCl + Py \rightleftarrows (TPP)MnPy^+ + Cl^- \quad (2)$$

$$Q = \frac{[(TPP)MnPy^+][Cl^-]}{[(TPP)MnCl][Py]} \quad (3)$$

equilibrium quotients ranging from $1.2 \times 10^{-3}$ to $4.1 \times 10^{-3}$ are calculated for 0.05 M and 0.25 M pyridine solutions, respectively. Variation in these values likely reflects deviation in Curie law behavior, which affects the accuracy of extrapolated room temperature coordinated chemical shifts. These $Q$ values are much smaller than those reported for electrochemical measurements at lower concentrations where the chloride term was seemingly ignored.[28]

Carbon-13 NMR measurements were also performed for solutions containing 0.03 M (TPP)MnCl and either 0.05, 0.10, or 0.25 M pyridine. Pyridine signals were relatively sharp, and chemical shifts were near those expected for the free ligand. Chemical shifts were surprisingly invariant with changes in pyridine concentration. For instance, the pyridine $\alpha$-carbon resonance moved only from 148.7 to 148.5 ppm for solutions containing 0.05 to 0.25 M pyridine. These observations can best be explained by a pyridine exchange rate, which is near the slow limit on the carbon-13 NMR time scale. The exchange rate for 4-methylpyridine with (TPP($p$-$OCH_3$))MnI must be somewhat more rapid, as 4-methylpyridine signals are broadened and shifted downfield (see Figure 4). For a $CDCl_3$ solution (at 34 °C) 0.04 M in (TPP($p$-$OCH_3$))MnI and 0.5 M in 4-methylpyridine the $\alpha$-carbon signal of pyridine is shifted 3 ppm downfield and the $\beta$-carbon is 15 ppm downfield from the free-ligand value. The greater shift for the $\beta$-carbon does not necessarily mean that the $\beta$-carbon signal is shifted further than the $\alpha$-carbon signal for coordinated pyridine. On the contrary, a relatively smaller shift would mean that bound and free ligand signals could begin to average. This explains the seemingly contradictory condition that ligand exchange is near the fast limit for pyridine deuterium signals but near the slow limit for carbon-13 resonances. A deuterium chemical shift difference of 106 ppm for bound and free pyridine translates into 1450 Hz (at 13.7 MHz). This means that the carbon-13 shift will have to be considerably greater (1450 Hz at 22.5 MHz is 65 ppm) to be in the near-slow-exchange limit. Chemical shifts for bound pyridine $\alpha$- and $\beta$-carbon atoms are thus expected to be hundreds of ppm downfield. These signals were not detected due to limited sensitivity and perhaps extreme broadening.

**Interpretation of Unpaired Spin Delocalization.** Patterns of d-orbital occupation are now well correlated with proton NMR shift patterns of paramagnetic metalloporphyrins.[1,2] Our understanding of carbon-13 NMR isotropic shifts is at an earlier stage of development, but the following statements may be made on the basis of the studies that have been reported. (1) Single occupation of the $\sigma$-interacting $d_{x^2-y^2}$ orbital is associated with pyrrole carbon resonances shifted to approximately 1000 ppm downfield.[6-10,17] (2) Uneven occupation of $\pi$-interacting $d_{xz}$, $d_{yz}$ ($d_{x^2-y^2}$ vacant) results in porphyrin core-carbon shifts that are generally upfield due to spin polarization in $\pi$-molecular orbitals and a large upfield ligand-centered dipolar shift term.[11-15] (3) Meso carbon signals may be far downfield due to involvement of the 4e($\pi^*$) molecular orbital which has large amplitude at the meso carbon atom or slightly upfield due to electron-correlation effects for the 3e($\pi$) molecular orbital.[10-15,17] (4) For TPP compounds with large meso carbon shifts, the ortho phenyl carbon shift parallels and the quaternary phenyl carbon shift is opposite to the meso carbon shift direction, perhaps due to a $\pi$–$\sigma$ spin polarization mechanism.[7,10] (5) When $\pi$-spin delocalization is important, pyrrole substituents also exhibit this extreme alternation in shift direction, with, for example, an ethyl group having an upfield $CH_2$ resonance and a downfield $CH_3$ resonance.[3,4,8,10-15,17] (6) Mixing of excited states may have profound effects on carbon-13 spectra and result in shift patterns characteristic of both ground and excited states.[18]

The $d_{xy}^1, d_{xz}^1, d_{yz}^1, d_{z^2}^1$ configuration of high-spin manganese(III) should be associated with a predominant $\pi$-spin delocalization mechanism for porphyrin resonances, as the $d_{x^2-y^2}$ orbital is vacant. Spectra in Figures 1 and 2 do indeed lack the approximately 1000 ppm pyrrole resonances apparent for high-spin iron(III) and high-spin iron(II) porphyrins. The presence of both upfield and downfield pyrrole carbon signals differs from the low-spin(III) example where both $\alpha$- and $\beta$-pyrrole carbon resonances are shifted upfield. Attempts to analyze manganese(III) isotropic shift values by the Karplus–Fraenkel relationship[15,33] yielded unreasonable, nearly zero spin densities at $\alpha$-pyrrole carbon atoms. The fact that manganese(III) is not amenable to such an analysis may implicate contribution of $\sigma$-spin density through the weakly interacting $d_{z^2}$ orbital. Alternately, the strong mixing of porphyrin and metal molecular orbitals, which is thought to be so important for manganese,[22] may upset the simple carbon-13 shift correlations made for other metalloporphyrins.

Additional qualitative statements may be made about the spin delocalization patterns. Rather small upfield shifts at meso carbon atoms are indicative of $\pi$-spin delocalization through the filled 3e($\pi$) molecular orbital via a porphyrin → manganese "back-bonding" mechanism. Appreciable negative spin density at the meso carbon position through electron correlation effects provides a reasonable explanation for the downfield shift of the meso proton signal for (OEP)MnCl and the downfield shift of the quaternary phenyl carbon of (TPP)MnCl derivatives. As the meso carbon signal is moved further upfield by 4-methylpyridine coordination, the attached quaternary phenyl and ortho phenyl signals behave as expected in moving further downfield and upfield, respectively. The shift patterns for alkyl pyrrole substituents of (OEP)MnCl and (ETIO)MnCl are consistent with a $\pi$-spin delocalization mechanism. In this instance the ring-$CH_3$ and -$CH_2$ signals are shifted upfield from $Me_4Si$ whereas the signal for a $CH_3$ group one carbon removed from the ring is far downfield (167 ppm).

Deuterium shift patterns for coordinated pyridine may be explained in a straightforward manner. The $\sigma$-interacting $d_{z^2}$ orbital is singly occupied and is directed toward the pyridyl nitrogen atom. Large downfield shifts for $\alpha$- and $\beta$-pyridine deuterium atoms (with some attenuation for the $\beta$-signal) are consistent with predominant $\sigma$-spin delocalization. A very small upfield shift for the $\gamma$-signal probably indicates measurable $\pi$-delocalization from a $\sigma$-$\pi$ spin polarization mechanism, or pyridine interaction with the $d_{xz}$,$d_{yz}$ set. The $\pi$-delocalization mechanism is predominant for the $\gamma$-deuterium atom, as the $\sigma$-effect is greatly attenuated at this distant site. Chemical shifts of 114 and 70 ppm of manganese(III) coordinated pyridine $\alpha$- and $\beta$-deuterium signals are to be compared with values of 70 and 36 ppm, respectivley, for the cobalt(II) complex.[18] The singly occupied $d_{z^2}$ orbital is utilized in both of these metal ions, whereas for low-spin iron(III), where the $\sigma$-interacting orbital is vacant, coordinated pyridyl proton chemical shifts are −8 ($\alpha$-H) and 11 ppm ($\beta$-H) (extrapolated from low temperature to 30 °C).[34]

Self-consistent charge-extended Hückel calculations have been performed for (TPP)MnCl.[35,36] Results indicate the

(33) Karplus, M.; Fraenkel, G. K. *J. Chem. Phys.* **1961**, *35*, 1312.
(34) La Mar, G. N.; Bold, T. J.; Satterlee, J. D. *Biochim. Biophys. Acta* **1977**, *498*, 189.

following unpaired spin densities at carbon atoms: α-pyrrole, 0.016; β-pyrrole, 0.017; meso, 0.019. Application of the Karplus-Fraenkel relationships to combined carbon-13 and proton NMR data could in principle be used to evaluate the theoretical predictions. Unfortunately, such calculations for the $S = 2$ system appear unreliable perhaps as a consequence of both σ- and π-spin delocalization mechanisms. Estimations of spin density at carbon atoms are possible, however, if it is assumed that the proton hyperfine coupling constant, $A^H$, is proportional to the unpaired spin density, $\rho_C^\pi$, centered on the π-orbital of the carbon atom to which it is attached.[33]

$$A^H = \frac{Q_{CH}{}^H \rho_C{}^\pi}{2S} \quad (4)$$

The empirical value of $Q_{CH}{}^H$ is taken as −63 MHz. The value for $A^H$ is obtained from the contact shift by (downfield shift given a positive sign)

$$\frac{\Delta H_{con}}{H} = A^H \frac{|\gamma_e|}{|\gamma_H|} \frac{S(S+1)}{3kT} \quad (5)$$

For contact shifts of −30.6 ppm (pyrrole H) and +41.4 ppm (meso H) previously reported by La Mar and Walker,[21] carbon spin density values of 0.0094 (β-pyrrole carbon) and −0.013 (meso carbon) are found. An extreme mismatch is apparent for the calculated meso carbon value and the theoretical prediction in that the signs are reversed. Further theoretical calculations that permit direct inclusion of electron correlation effects are clearly needed.

**Acknowledgment.** We gratefully acknowledge support from the National Science Foundation, Grant CHE 79-10305.

**Registry No.** (TPP)MnCl, 32195-55-4; (TPP(*m*-$CH_3$))MnCl, 56811-40-6; (TPP(*p*-$OCH_3$))MnCl, 62769-24-8; (TPP(*p*-$OCH_3$))MnI, 88271-89-0; (TPP(*p*-$OCH_3$))MnF, 88271-90-3; (TPP(*p*-$OCH_3$))Mn(4-MePy)$^+$, 88271-91-4; (OEP)MnCl, 28265-17-0; (ETIO)MnCl, 58675-99-3.

(35) Mun, S. K.; Mallick, M. K.; Mishra, S.; Chang, J. C.; Das, T. P. *J. Am. Chem. Soc.* **1981**, *103*, 5024.
(36) Mishra, S.; Chang, J. C.; Das, T. P. *J. Am. Chem. Soc.* **1980**, *102*, 2674.

Contribution from the Department of Chemistry, University of California, Davis, California 95616

# A Nickel Complex Containing an Extremely Long Nickel-Phosphorus Bond. Syntheses and X-ray Structures of $[Ni(CN)_2[P(CH_2OH)Ph_2]_3](C_6H_6)_{0.5}$ and *trans*-$[Ni(CN)_2[P(CH_2OH)Ph_2]_2]$

H. HOPE, M. M. OLMSTEAD, P. P. POWER,* and M. VIGGIANO

*Received March 16, 1983*

The syntheses and crystal and molecular structures of two derivatives of Ni(II) with (hydroxymethyl)diphenylphosphine, a potentially bidentate ligand, are reported. These compounds are dicyanotris((hydroxymethyl)diphenylphosphine)nickel(II)-0.5-benzene ($[Ni(CN)_2[P(CH_2OH)Ph_2]_3](C_6H_6)_{0.5}$, **1**) and *trans*-dicyanobis((hydroxymethyl)diphenylphosphine)nickel(II) (*trans*-$[Ni(CN)_2[P(CH_2OH)Ph_2]_2]$, **2**). Complex **1**, which was synthesized in good yield by the reaction of $Na_2[Ni(CN)_4]\cdot 3H_2O$ with $PHPh_2$ and aqueous formaldehyde in benzene solution at 60 °C, crystallizes as red needles, space group $P\bar{1}$ (No. 2), unit cell dimensions $a = 12.323$ (9) Å, $b = 12.844$ (10) Å, $c = 15.507$ (10) Å, $\alpha = 111.38$ (5)°, $\beta = 90.39$ (6)°, $\gamma = 119.85$ (6)°, $Z = 2$. The structure has been refined to an $R$ index of 0.057 on the basis of 2855 unique reflections. The potentially bidentate ligand coordinates through phosphorus only. The inner coordination about nickel is closer to square-pyramidal than to trigonal-bipyramidal geometry. The metal is coordinated to three phosphorus and two cyano carbon atoms. One of the Ni-P bonds is extremely long, with a Ni-P distance of 2.400 (3) Å. Complex **1** readily dissociates a phosphine under mild conditions to afford **2** in quantitative yield. The structure of **2** has the simple trans-square-planar geometry at nickel. The orange-yellow crystals belong to the orthohombic space group *Pbca* (No. 61) with unit cell dimensions $a = 10.258$ (2) Å, $b = 16.173$ (5) Å, $c = 15.055$ (3) Å, and $Z = 4$. The structure has been refined to $R = 0.038$ on the basis of 1765 unique reflections. The Ni-P bond lengths are normal, and there is no interaction between the OH groups and the metal atom. The free ligand $P(CH_2OH)Ph_2$ may be isolated in ca. 70% yield from either complex by treatment with excess $CN^-$ in aqueous solution.

## Introduction

We are currently interested in ligands of the type $P(CH_2X)Ph_2$ where X = OH, SH, NHR, or PHR, and R = alkyl or aryl group. These ligands can behave as uninegative or neutral mono- or bidentate donors. Our initial work has concentrated on the ligand $P(CH_2OH)Ph_2$. A previous report has dealt with some rhodium, palladium, and platinum complexes,[1] but no structure of any complex involving this ligand has appeared.

In this paper we report the first X-ray crystal structures of such complexes. In addition, we describe a novel high-yield synthetic route involving the reaction of a metal salt with a secondary phosphine in the presence of aqueous formaldehyde.

## Experimental Section

**Materials.** Sodium tetracyanonickelate trihydrate was synthesized according to literature procedures.[2] Diphenylphosphine (Strem), formaldehyde (37% in water), benzene, and sodium cyanide (Mallinckrodt) were used as purchased.

**Preparation and Characterization of Complexes.** All syntheses were performed under an atmosphere of nitrogen with modified Schlenk techniques. Both products **1** and **2** are air-stable crystalline materials, but **1** dissociates to **2** and free ligand at room temperature in solvents such as $C_6H_6$ or $CHCl_3$. $^1H$ NMR spectra were recorded on a Varian EM-390 spectrometer and $^{31}P$ NMR spectra on a Nicolet NT-200

(1) Chatt, J.; Leigh, J.; Slade, R. M. *J. Chem. Soc., Dalton Trans.* **1973**, 2021-2028.
(2) Fernelius, W. C.; Burbage, J. J. *Inorg. Synth.* **1946**, *2*, 227-228. McCullough, R. L.; Jones, L. H.; Crosby, G. A. *Spectrochim. Acta* **1960**, *16*, 929-944.

0020-1669/84/1323-0326$01.50/0 